Cross-Coupling Reactions

DOI: 10.1002/ange.200703978

Synthesis and Characterization of Expanded Radialenes, Bisradialenes, and Radiaannulenes**

*Mojtaba Gholami, Frederic Melin, Robert McDonald, Michael J. Ferguson, Luis Echegoyen, and Rik R. Tykwinski**

Shape-persistent, conjugated macrocycles have been designed to exhibit a broad spectrum of interesting attributes and topologies.[1] Over the past two decades amazing progress has been made towards the synthesis of these macrocycles, which have remarkable electronic, optical, nonlinear optical, and supramolecular properties.[2–4] A subset of this general class of molecules are the radialenes (**1**) and expanded radialenes (**2** and **3**; see Scheme 1), which arise from the formal insertion of acetylene units into the framework of a radialene molecule.[5] A related class of macrocycles, radiaannulenes (**4**, Scheme 1), contain both endo- and exocyclic vinyl segments within the conjugated core.[6] Both the expanded radialenes and the radiaannulenes are cross-conjugated macrocycles,[3,4] and their rigid two-dimensional structure provides a useful framework for the development of fundamentally interesting π-rich molecules. The study of expanded radialenes was initiated by Diederich and co-workers,[7] who explored the rich chemistry of butadiynyl-based radialenes **3** and radiaannulenes **4**. These studies, and others, used a combination of functional group variation and extensive analysis of their physical properties, and have suggested that molecules such as **3** and **4** can be generated with intriguing optical and electronic properties.[3,4] Radialenes **2** would be expected to share many of the attractive electronic characteristics of their larger cousins **3**.

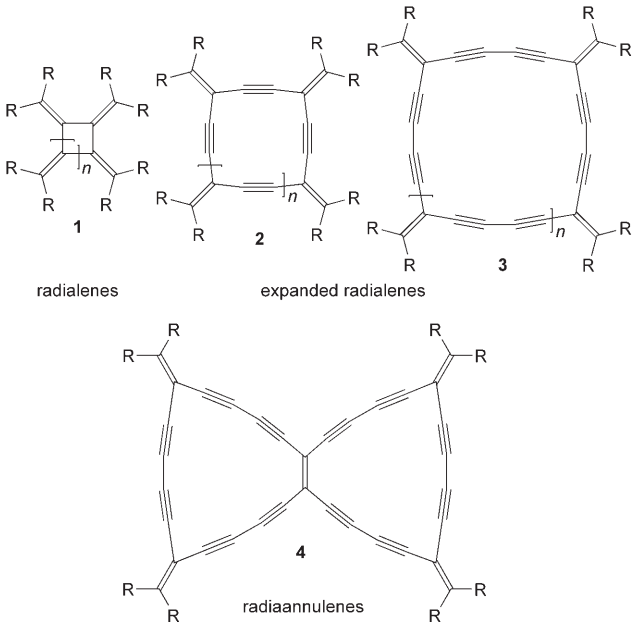

Scheme 1. Structures of radialenes, expanded radialenes, and radiaannulenes.

Furthermore, a recent computational study has suggested that upon a single-electron reduction, a trimeric derivative of **2** ($n = 0$) should become antiaromatic.[8] To date, however, the synthesis of radialenes **2** has proved challenging, and only a single example has been reported (**2**, $n = 3$, R = alkyl).[9]

Herein, we report a general protocol for the synthesis of expanded radialenes **5**–**8** from acyclic oligomers **9**–**12** and vinyl bromide **13** (Scheme 2). Also described are our initial efforts to extend this method through coupling with tetrabromoethane (**14**) to generate the first examples of enyne bisradialenes, namely **15** and **18**, and radiaannulenes, namely **16** and **17**. Finally, the structural (X-ray crystallography), electronic (cyclic voltammetry), and optical (absorbance and emission) properties of the isolated macrocycles **5**–**7**, **15**/**16**, and **17** are described.

The new expanded radialenes were synthesized from enyne oligomers **9**–**12**,[10] which were desilylated and then reacted with **13** under Pd-catalyzed Sonogashira conditions (Scheme 2).[11] For example, dimer **9** was desilylated with tetra-*n*-butylammonium fluoride (TBAF) in wet THF to give the terminal diyne. Following workup, the diyne was then reacted with **13** in the presence of $[Pd(PPh_3)_4]$, CuI, and iPr_2NH in THF at reflux to give the highly strained expanded [3]radialene **5** in a reasonable yield of 32%. The successful ring closure to give **5** provides a noteworthy achievement of

[*] M. Gholami, Prof. Dr. R. R. Tykwinski
Department of Chemistry
University of Alberta
Edmonton, AB, T6G 2G2 (Canada)
Fax: (+1) 780-492-8231
E-mail: rik.tykwinski@ualberta.ca
Dr. F. Melin, Prof. Dr. L. Echegoyen
Department of Chemistry
Clemson University
Clemson, South Carolina, 29634 (USA)
E-mail: luis@clemson.edu
Dr. R. McDonald, Dr. M. J. Ferguson
X-ray Crystallography Laboratory
Department of Chemistry
University of Alberta
Edmonton, Alberta, T6G 2G2 (Canada)

[**] The financial support provided by the University of Alberta, the Natural Sciences and Engineering Research Council of Canada (NSERC), and the National Science Foundation (grant number CHE-0509989) is greatly appreciated. This material is based on work supported by the National Science Foundation while L.E. was working here. All opinions, findings, conclusions, and recommendations expressed herein are those of the authors and do not necessarily reflect the views of the National Science Foundation.

Supporting information for this article is available on the WWW under http://www.angewandte.org or from the author.

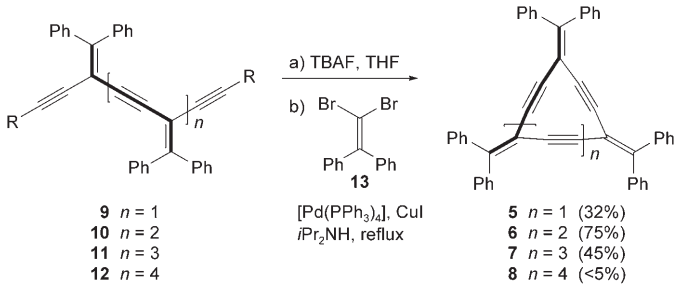

Scheme 2. Synthesis of expanded radialenes **5**–**8** (the linearly conjugated ene-yne-ene segment is highlighted in bold). R = $SiMe_2tBu$.

the Sonogashira reaction to effect bond formation in an incredibly strained cyclic system.[12]

Based on the same strategy, trimer **10** and tetramer **11** were used in a similar manner to synthesize [4]- and [5]radialenes **6** and **7** in yields of 75 and 45%, respectively. Attempts to form the analogous [6]radialene **8**, however, resulted in only very poor yields, with the macrocycle derived from the intramolecular oxidative acetylenic homocoupling[13] of desilylated **12** being isolated as the major product (64%).[14] The difficulty in forming **8** most likely arises from the significant steric crowding originating from the 12 pendent phenyl rings, which reduces the ability of this macrocycle to approach the approximately planar conformation that would favor ring closure.

Spectroscopically, all three radialenes **5**–**7** share the common feature of only seven unique resonances in their ^{13}C NMR spectra as a result of their symmetry. Of note is the consistent shift of particular resonances as a result of the increased ring strain, as has been noted for other acetylenic macrocycles.[15] For example, the resonance of the exocyclic vinylidene carbon atom is the most diagnostic, and this signal shifts upfield from $\delta = 155$ ppm for [5]radialene **7** to $\delta =$ 146 ppm for the most strained [3]radialene **5**.

Carbon-rich, highly conjugated bisexpanded radialene and radiaannulene compounds were then prepared through a single-step reaction of the corresponding enyne precursor with tetrabromoethene (**14**, Scheme 3). Thus, trimeric **10** was desilylated and treated with **14** for 18 h under conditions analogous to those for the synthesis of radialenes **5**–**7**. Separation of the major reaction product by chromatography gave an orange solid that MALDI-TOF mass spectrometric (MS) analysis showed was consistent with the expected product(s) **15** and/or **16**. ^{13}C NMR spectroscopic analysis of this material showed that more than one product was present, but gave little indication of which compound had formed preferentially. Unfortunately, all subsequent attempts to separate the isomers were unsuccessful, although HPLC analysis showed an approximate 2:1 ratio of products.[14] X-ray crystallography ultimately confirmed bisradialene **15** was likely to be the predominant product (see below).

Desilylation of dimeric **9**, followed by treatment with **14** gave a dark red-purple solid (Scheme 4), which MALDI-TOF MS data indicated was consistent with the formation of product(s) **17** and/or **18**. Although this solid was only poorly soluble in common organic solvents, thus making purification a challenge, separation by preparative TLC did provide a pure

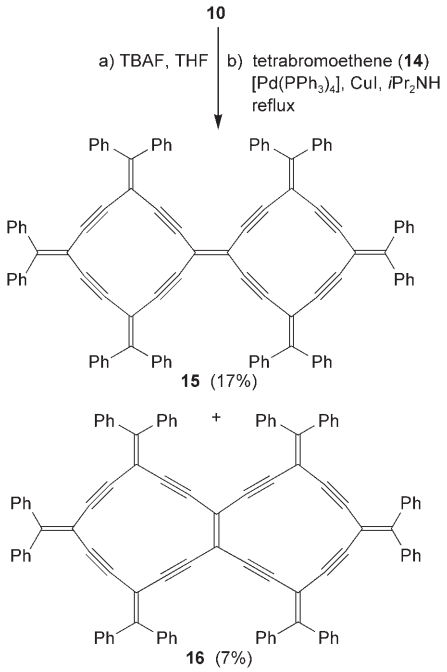

Scheme 3. Synthesis of expanded bisradialene **15** and radiaannulene **16**.

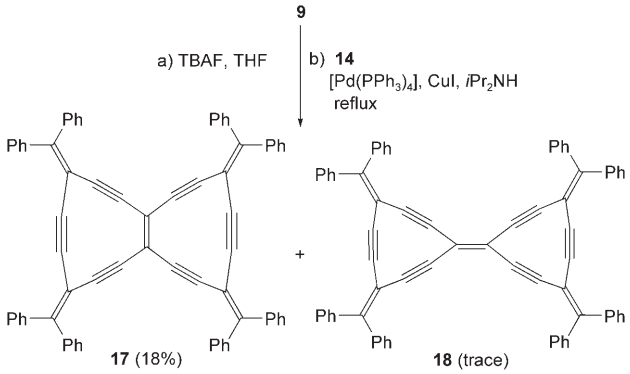

Scheme 4. Synthesis of expanded radiaannulene **17** and bisradialene **18**.

product in 18% yield. ^{13}C NMR spectroscopic analysis of this product identified 13 resonances (out of the 14 expected), which were consistent with the structure of either **17** or **18**. The constitution of the product was ultimately confirmed to be **17** by X-ray crystallography (see below). A trace amount of a second product was tentatively identified as **18** on the basis of MALDI-TOF MS analysis.

The absorption spectra of the expanded radialenes **5**–**7** were measured in THF at room temperature.[16] The spectra of **6** and **7** show a single strong absorption at $\lambda_{max} = 377$ nm ($\varepsilon =$ 99300 $L\,mol^{-1}\,cm^{-1}$) and $\lambda_{max} = 374$ nm ($\varepsilon =$ 51300 $L\,mol^{-1}\,cm^{-1}$), respectively, with a much weaker shoulder absorption for **6** at approximately 420 nm. The major difference between radialenes **6** and **7** is the lower molar absorptivity of **7**, which may arise from its more flexible and nonplanar structure. Conversely, [3]radialene **5** shows two major maxima at $\lambda_{max} = 364$ nm ($\varepsilon = 105300$ $L\,mol^{-1}\,cm^{-1}$)

and 415 nm ($\varepsilon = 107\,500\ \mathrm{L\,mol^{-1}\,cm^{-1}}$). At present, the origin of the more significant lower energy absorption for **5** is not yet understood. It may be the result of an augmentation of the shoulder signal observed for **6** as a result of the decreased conformational flexibility in the more strained structure of **5**. Conversely, it may arise from an increase in macrocyclic cross-conjugation, which has been invoked to account for the red shift in the λ_{max} values observed for trimeric derivatives of the larger expanded radialenes **3**.[4,17] The latter argument is supported through a comparison of the λ_{max} values for **5–7** with those of the acyclic precursors **9–11**, which show $\lambda_{max} =$ 374 nm when measured in THF.[10,18] Since the longest linearly conjugated segment is identical in **5–7** and **9–11** (shown in bold in Scheme 2), the low-energy absorption of **5** must arise from other factors.[19]

The high-energy region of the absorption spectrum of radiaannulene **17** shows an absorption similar to that of radialenes **5–7** (at $\lambda_{max} = 381$ nm, $\varepsilon = 63\,000\ \mathrm{L\,mol^{-1}\,cm^{-1}}$).[16] The low-energy region is, however, quite dissimilar from those of **5–7** and shows two additional maxima at $\lambda_{max} =$ 534 nm ($\varepsilon = 19\,500\ \mathrm{L\,mol^{-1}\,cm^{-1}}$) and 572 nm ($\varepsilon = 31\,700\ \mathrm{L\,mol^{-1}\,cm^{-1}}$), which signify a substantial lowering of the gap between the highest occupied molecular orbital and lowest unoccupied molecular orbital (HOMO–LUMO). It is unlikely that this lowering of the HOMO–LUMO gap derives simply from an extension of the linearly conjugated segment of **17**, since the oligodiacetylene **19**, synthesized by Giesa and

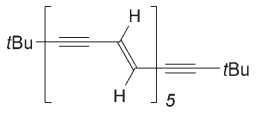

19

Schulz, shows $\lambda_{max} = 418$ nm; which is over 100 nm higher in energy than that of radiaannulene **17** despite its longer linear conjugated segment.[20] Thus, it seems clear that the constrained, cross-conjugated framework of **17** plays a major role in the electronic makeup of this compound.

While isomers **15** and **16** could not be separated to allow for UV/Vis analysis of each isomer individually, an empirical comparison to **17** is nonetheless interesting. The mixture of **15** and **16** shows the same high-energy absorption maximum at 387 nm as found for **17**, as well as a single broadened low-energy absorption maximum at 509 nm, albeit blue shifted versus that of **17**. Thus, the mixture of **15** and **16** also seems to exhibit unique electronic characteristics resulting from their macrocyclic structure.

The fluorescence spectra of compounds **5–7** ($\lambda_{exc} =$ 380 nm, THF, room temperature) show a single broad emission peak (λ_{em}) with similar relative intensities. The observed Stokes shift increases as a function of the size of the macrocycle (λ_{em}: **5**: 498 nm, **6**: 525 nm, **7**: 544 nm), and can be attributed to increased molecular flexibility in the larger cycles. Compound **17** shows an intense emission at $\lambda_{em} =$ 594 nm, and the emission wavelength does not vary as a function of the excitation wavelength ($\lambda_{exc} = 380$, 533, or 571 nm).

The electrochemical properties of **5–7** and **17** were measured in CH_2Cl_2 containing 0.1 M nBu_4PF_6 and with a 3-mm diameter glassy carbon disk as the working electrode (Figure 1). Ferrocene was added at the end of the experiments and used as an internal reference for measuring the potentials. Despite the different size of their cross-conjugated macro-

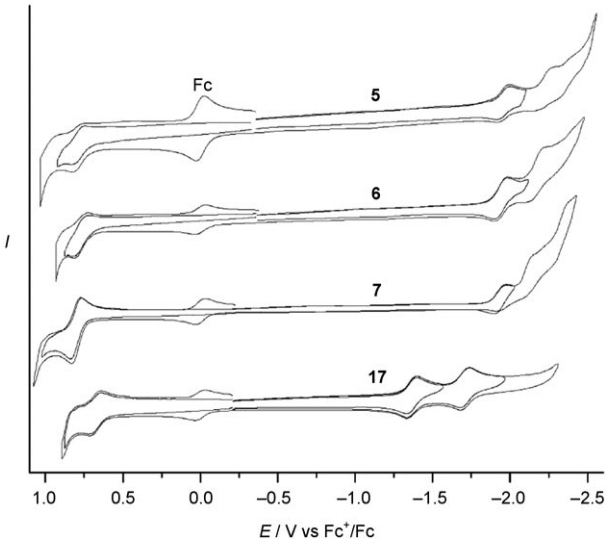

Figure 1. Cyclic voltammagrams of radialenes **5–7** and radiaannulene **17** measured in CH_2Cl_2 + 0.1 M nBu_4PF_6 (scan rate 100 $mV\,s^{-1}$). Fc^+/Fc = ferrocenium/ferrocene couple.

cyclic framework, expanded radialenes **5–7** showed comparable redox behavior. For these three compounds two reduction steps were observed, the first reversible at −2.0 V versus Fc^+/Fc and the second was less well defined at −2.2 V versus Fc^+/Fc. A single, one-electron, reversible oxidation step at 0.8 V was also observed (Table 1). Therefore, no significant lowering of the electrochemical HOMO–LUMO gap was observed for compound **5**, despite its lower energy absorption in the UV/Vis region. The same trend was found for the larger expanded radialenes **3**, as described by Diederich and co-workers, where similar redox potentials were observed irrespective of the size of the macrocycle ($n = 1$–3).[21] The smaller radialenes **5–7** are considerably more difficult to reduce than any of the reported radialenes **3**.[17,21] The difficult reduction of compound **5** may substantiate the prediction of Chauvin and co-workers[8] that a one-electron reduction of a [3]radialene analogue to **5** (i.e., **2** $n = 0$, R = H) should lead to an antiaromatic molecule, although this premise inspires the analysis of additional substitution patterns (which is currently under investigation). In contrast to **5–7**, radiannulene **17** was both easier to reduce and oxidize,

Table 1: Peak and half-wave potentials of the first reduction and oxidation steps of expanded radialenes **5–7** and radiaannulene **17**.

Cmpd	Ep_c red.$_1$	Ep_a red.$_1$	$E_{1/2}$ red.$_1$	Ep_a ox.$_1$	Ep_c ox.$_1$	$E_{1/2}$ ox.$_1$
5	−1.99	−1.92	−1.96	0.82	0.75	0.79
6	−1.98	−1.91	−1.94	0.81	0.75	0.78
7	−1.98	−1.91	−1.94	0.83	0.76	0.80
17	−1.40	−1.33	−1.36	0.71	0.64	0.68

which is consistent with the UV/Vis absorption data that showed a smaller HOMO–LUMO gap for **17**. Compound **17** presented two reversible one-electron reductions at −1.36 V and −1.71 V versus Fc^+/Fc and a reversible one-electron oxidation at 0.68 V versus Fc^+/Fc.

Single crystal X-ray analysis of **6** (Figure 2) shows a planar cyclic core, with the pendent phenyl groups twisted from this plane in a manner that facilitates π–π stacking interactions. In contrast, the structure of **7** is not planar,[14] and its cyclic core resembles an envelope conformation, which likely arises from increased steric interactions between the pendent phenyl rings.

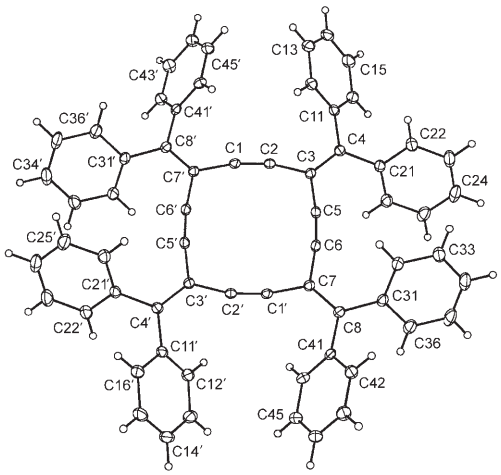

Figure 2. ORTEP drawing of radialene **6**. Thermal ellipsoids are drawn at the 20% probability level. Selected bond angles [°]: C2-C1-C7′ 168.23(14), C1-C2-C3 166.65(14), C2-C3-C5 110.40(12), C3-C5-C6 172.20(15), C5-C6-C7 171.30(15), C1′-C7-C6 110.40(11).

A comparison of structures **6** and **7** confirms the increased strain found in the former. While bond lengths for both fall within similar ranges, the bond angles within the macrocyclic cores differ quite dramatically. The C≡C–C bond angles for **6** range from 166.7° to 172.2° (average: 169.6°), while those for **7** range from 171.0° to 177.4° (average: 173.7°). The endocyclic alkylidene bond angles also show the effect of ring strain, with both unique angles of **6** observed at 110.4°, and those of **7** ranging from 111.7° to 113.5° (average: 112.6°).

Crystals of radiaannulene **17** were grown from THF/pentane at 4–5 °C and X-ray analysis shows that the cyclic core of this molecule adopts a planar geometry (Figure 3). The endocyclic alkylidene bond angles C7–C8–C10 at 105.7(3)° and C3–C4–C6 at 106.9(3)° are significantly smaller than those observed for either **6** or **7** and reflect the significant ring strain in the framework. The alkyne bond angles of **17** are also substantially reduced from optimal values, and range from 158.1(3)° to 173.6(4)° (average: 164.6°).

Bisradialene **15** and radiaannulene **16** cocrystallize from $CHCl_3$ and with various ratios of the two molecules in the crystalline state depending on the initial sample (in the structure shown here, a **15**:**16** ratio of 2:1 is observed, Figure 4). The two structures are remarkably similar, and while they are disordered about the central tetraethynyl-

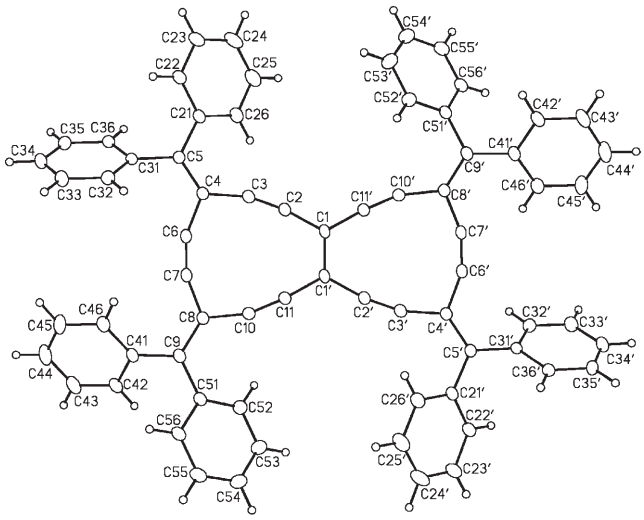

Figure 3. ORTEP drawing of radiaannulene **17.** Thermal ellipsoids are drawn at the 20% probability level. Selected bond angles [°]: C1′-C1-C11′ 119.7(4), C2-C1-C11′ 122.3(3), C1′-C1-C2 118.0(4), C1-C2-C3 171.0(4), C2-C3-C4 164.2(4), C3-C4-C6 106.9(3), C4-C6-C7 158.1(3), C6-C7-C8 159.6(3), C7-C8-C10 105.7(3), C8-C10-C11 161.1(4), C1′-C11-C10 173.6(4).

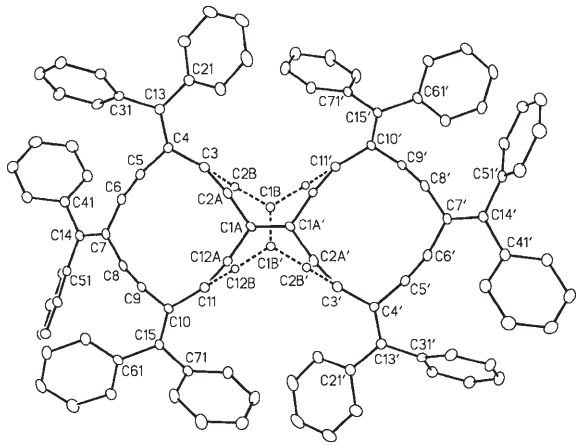

Figure 4. ORTEP drawing illustrating both the structure and disorder of the cocrystallite formed from bisradialene **15** and radiaannulene **16**. Thermal ellipsoids are drawn at the 20% probability level. Selected bond angles [°]: C1A-C2A-C3 172.6(9), C2A-C3-C4 160.4(6), C1A-C12A-C11 172.7(9), C1B-C2B-C3 174.6(19), C2B-C3-C4 175.2(10), C1B′-C12B-C11 178.9(16), C10-C11-C12B 175.8(9), C3-C4-C5 109.8(3), C4-C5-C6 170.3(3), C5-C6-C7 167.1(3), C6-C7-C8 109.9(3), C7-C8-C9 165.4(3), C8-C9-C10 171.3(3), C9-C10-C11 110.9(3), C10-C11-C12A 160.6(5).

ethenes core in the solid state, the spatial arrangement of the remaining atoms of the structure is shared by both molecules.

Unlike **17**, neither **15** nor **16** are planar: both have a stretched chair conformation.[14] The structure of **15** shares many similarities to that of [4]radialene **6**, including C≡C–C bond angles that average 167.6° (range: 160.4° to 172.7°). Radiaannulene **16** is the next higher analogue of **17**, and shows substantially less ring strain than **17** with an average bond angle of 172.3° (range: 165.5° to 178.9°) and also internal alkylidene bond angles that are between 110 and 111°. A comparison of the bond angles for structures **15** and **16** shows that the bisradialene is clearly the more strained of the two.

In conclusion, the synthesis of a new class of stable expanded radialenes and radiaannulenes has been demonstrated. This study has shown that macrocycles with incredibly strained conjugated enyne structures can be synthesized by Sonogashira cross-coupling reactions. UV/Vis absorption spectroscopy indicates that the electronic characteristics of the expanded radialenes are related to their macrocyclic cross-conjugated framework, and that the more strained the structure, the more interesting the electronic properties. A study of the fundamental structure–property relationships for these and related compounds is currently underway.

Experimental Section

5: Yellow solid. M.p. 185–186 °C; UV/Vis (THF): λ_{max} (ε L mol^{-1} cm^{-1}) 364 (105300), 415 nm (107500); IR (CH_2Cl_2, cast): $\tilde{\nu}$ = 3055 cm^{-1}; ^{1}H NMR (400 MHz, CD_2Cl_2): δ = 7.61–7.57 (m, 12H), 7.42–7.39 ppm (m, 18H); ^{13}C NMR (125 MHz, CD_2Cl_2): δ = 146.2, 139.7, 130.7, 129.5, 128.3, 107.2, 92.5 ppm. EI HRMS calcd for $C_{48}H_{30}$ [M^+]: 606.2347, found: 606.2354.

6: Yellow solid. M.p. 305–306 °C (decomp); UV/Vis (THF): λ_{max} (ε L mol^{-1} cm^{-1}) 377 nm (99300); IR (CH_2Cl_2, cast): $\tilde{\nu}$ = 3050 cm^{-1}; ^{1}H NMR (400 MHz, $CDCl_3$): δ = 7.26–7.16 (m, 24H), 7.08 ppm (t, J = 6.6 Hz, 16H); ^{13}C NMR (125 MHz, CD_2Cl_2): δ = 151.8, 140.1, 130.2, 129.1, 128.3, 102.6, 97.1 ppm; MALDI-TOF MS (*trans*-2-(3-(4-tert-butylphenyl)-2-methyl-2-propenylidene)malononitrile, DCTB) calcd for $C_{64}H_{40}$ [M^+]: 808.3, found: 808.2 (100).

7: Yellow solid. M.p. 300–301 °C (decomp); UV/Vis (THF): λ_{max} (ε L mol^{-1} cm^{-1}) 374 nm (51300); IR (CH_2Cl_2, cast): $\tilde{\nu}$ = 3051 cm^{-1}; ^{1}H NMR (300 MHz, $CDCl_3$): δ = 7.18–7.13 (m, 30H), 7.08 ppm (t, J = 7.2 Hz, 20H); ^{13}C NMR (125 MHz, CD_2Cl_2): δ = 155.2, 140.4, 130.6, 129.3, 128.1, 101.9, 90.7 ppm; MALDI-TOF MS (DCTB) calcd for $C_{80}H_{50}$ [M^+]: 1010.4, found: 1010.4 (100).

17: Red-purple solid. M.p. 250–251 °C (decomp); UV/Vis (THF): λ_{max} (ε L mol^{-1} cm^{-1}) 381 nm (63000), 534 nm (19500), 572 nm (31700); IR (CH_2Cl_2, cast): $\tilde{\nu}$ = 3057, 2141 cm^{-1}; ^{1}H NMR (300 MHz, $CDCl_3$): δ = 7.54–7.30 ppm (m, 40H); ^{13}C NMR (125 MHz, CD_2Cl_2): δ = 149.0, 139.7, 139.4, 130.8, 130.6, 129.8, 129.7, 128.4, 128.3, 104.4, 102.9, 101.5, 96.0 ppm (one resonance was not observed). MALDI-TOF MS (DCTB) calcd $C_{70}H_{40}$for [M^+]: 880.3, found: 880.2 (100).

15 and **16**: Orange solid. M.p. 295–296 °C (decomp); UV/Vis (THF): λ_{max} (ε L mol^{-1} cm^{-1}) 387 nm (139400), 509 nm (38900); IR (CH_2Cl_2, cast): $\tilde{\nu}$ = 3052, 2153, 1442 cm^{-1}. MALDI-TOF MS (DCTB) calcd for $C_{102}H_{60}$ [M^+]: 1285.5, found: 1285.5 (100).

Crystallographic data for **6**: $C_{64}H_{40}\cdot 2\,C_4H_8O$, M_r = 953.17, triclinic, space group $P\bar{1}$ (no. 2); a = 7.1300(5), b = 10.7812(8), c = 17.0015(12) Å; α = 78.4123(14), β = 89.7067(15), γ = 85.7118(14)°; V = 12762.62 (16) Å^3; Z = 1; ρ_{calcd} = 1.240 g cm^{-3}; μ = 0.073 mm^{-1}; T = −80 °C; $R_1(F)$ = 0.0478 (3382 reflections $F_o^2 \geq 2\sigma(F_o^2)$) and wR_2 = 0.1267 for all 5189 unique data.

Crystallographic data for **7**: $C_{80}H_{50}$, M_r = 1011.20, monoclinic, space group $P2_1/n$ (an alternate setting of $P2_1/c$ (no. 14)); a = 16.5917(10), b = 16.7378(10), c = 20.4413(12) Å; β = 90.5758(12)°; V = 5676.4(6) Å^3; Z = 4; ρ_{calcd} = 1.183 g cm^{-3}; μ = 0.067 mm^{-1}; T = −80 °C; $R_1(F)$ = 0.0514 (6933 reflections $F_o^2 \geq 2\sigma(F_o^2)$) and wR_2 = 0.1381 for all 11629 unique data.

Crystallographic data for **15** and **16**: $C_{102}H_{60}\cdot 3\,CHCl_3$, M_r = 1643.60, triclinic, space group $P\bar{1}$ (no. 2); a = 9.1206(9), b = 13.8110(13), c = 17.4081(17) Å; α = 98.2298(16), β = 93.2189(16), γ = 106.1213(16)°; V = 2074.2(3) Å^3; Z = 1; ρ_{calcd} = 1.316 g cm^{-3}; μ = 0.354 mm^{-1}; T = −80 °C; $R_1(F)$ = 0.0835 (5020 reflections $F_o^2 \geq 2\sigma(F_o^2)$) and wR_2 = 0.2758 for all 7288 unique data.

Crystallographic data for **17**: $C_{70}H_{40}$, M_r = 881.02, orthorhombic, space group *Pbca* (no. 61); a = 27.982(6), b = 19.339(4), c = 9.028(2) Å; V = 4885.5(19) Å^3; Z = 4; ρ_{calcd} = 1.198 g cm^{-3}; μ = 0.068 mm^{-1}; T = −80 °C; $R_1(F)$ = 0.0619 (2135 reflections $F_o^2 \geq 2\sigma(F_o^2)$) and wR_2 = 0.1837 for all 4304 unique data. CCDC-652685 (**6**), 652686 (**7**), 652687 (**15** and **16**), and 652688 (**17**) contain the supplementary crystallographic data for this paper. These data can be obtained free of charge from The Cambridge Crystallographic Data Centre via www.ccdc.cam.ac.uk/data_request/cif.

Received: August 29, 2007
Published online: October 26, 2007

Keywords: cross-conjugation · cross-coupling · macrocycles · radiaannulenes · radialenes

[1] a) W. Zhang, J. S. Moore, *Angew. Chem.* **2006**, *118*, 4524 – 4548; *Angew. Chem. Int. Ed.* **2006**, *45*, 4416 – 4439; b) K. Tahara, Y. Tobe, *Chem. Rev.* **2006**, *106*, 5274 – 5290; c) E. L. Spitler, C. A. Johnson II, M. M. Haley, *Chem. Rev.* **2006**, *106*, 5344 – 5386; d) C. Grave, A. D. Schlüter, *Eur. J. Org. Chem.* **2002**, 3075 – 3098.
[2] a) S. Höger in *Acetylene Chemistry* (Eds.: F. Diederich, P. J. Stang, R. R. Tykwinski), Wiley-VCH, Weinheim, **2005**, Chapter 10; b) Y. Yamaguchi, Z. Yoshida, *Chem. Eur. J.* **2003**, *9*, 5430 – 5440; c) U. H. F. Bunz, *J. Organomet. Chem.* **2003**, *683*, 269 – 2876.
[3] M. Gholami, R. R. Tykwinski, *Chem. Rev.* **2006**, *106*, 4997 – 5027.
[4] M. B. Nielsen, F. Diederich, *Chem. Rev.* **2005**, *105*, 1837 – 1867.
[5] H. Hopf, G. Maas, *Angew. Chem.* **1992**, *104*, 953 – 977; *Angew. Chem. Int. Ed. Engl.* **1992**, *31*, 931 – 954.
[6] F. Mitzel, C. Boudon, J. P. Gisselbrecht, P. Seiler, M. Gross, F. Diederich, *Helv. Chim. Acta* **2004**, *87*, 1130 – 1157.
[7] J. Anthony, A. M. Boldi, C. Boudon, J.-P. Gisselbrecht, M. Gross, P. Seiler, C. B. Knobler, F. Diederich, *Helv. Chim. Acta* **1995**, *78*, 797 – 817.
[8] C. Lepetit, M. B. Nielsen, F. Diederich, R. Chauvin, *Chem. Eur. J.* **2003**, *9*, 5056 – 5066.
[9] S. Eisler, R. R. Tykwinski, *Angew. Chem.* **1999**, *111*, 2138 – 2141; *Angew. Chem. Int. Ed.* **1999**, *38*, 1940 – 1943.
[10] Y. Zhao, A. D. Slepkov, C. O. Akoto, R. McDonald, F. A. Hegmann, R. R. Tykwinski, *Chem. Eur. J.* **2005**, *11*, 321 – 329.
[11] a) K. Sonogashira, Y. Tohda, N. Hagihara, *Tetrahedron Lett.* **1975**, *16*, 4467 – 4470; b) R. R. Tykwinski, *Angew. Chem.* **2003**, *115*, 1604 – 1606; *Angew. Chem. Int. Ed.* **2003**, *42*, 1566 – 1568.
[12] The C≡C–C bond angles for **5** are calculated to be 158°: AM1 geometry minimization, Spartan'02 v1.0.6, Wavefunction, Inc.
[13] P. Siemsen, R. C. Livingston, F. Diederich, *Angew. Chem.* **2000**, *112*, 2740 – 2767; *Angew. Chem. Int. Ed.* **2000**, *39*, 2632 – 2657.
[14] See the Supporting Information for details.
[15] S. Eisler, R. McDonald, G. R. Loppnow, R. R. Tykwinski, *J. Am. Chem. Soc.* **2000**, *122*, 6917 – 6928.
[16] See the Supporting Information for spectra.
[17] M. B. Nielsen, M. Schreiber, Y. G. Baek, P. Seiler, S. Lecomte, C. Boudon, R. R. Tykwinski, J.-P. Gisselbrecht, V. Gramlich, P. J. Skinner, C. Bosshard, P. Günter, M. Gross, F. Diederich, *Chem. Eur. J.* **2001**, *7*, 3263 – 3280.
[18] C. A. Lewis, R. R. Tykwinski, *Chem. Commun.* **2006**, 3625 – 3627.
[19] It is possible that molecular symmetry and the associated selection rules also contribute to the differences observed in the electronic transitions of **5**–**7**, as has recently been outlined for cyclic oligothiophenes, see A. Bhaskar, G. Ramakrishna, K. Hagedorn, O. Varnavski, E. Mena-Osteritz, P. Bäuerle, T. Goodson III, *J. Phys. Chem. B* **2007**, *111*, 946 – 954.
[20] R. Giesa, R. C. Schulz, *Polym. Int.* **1994**, *33*, 43 – 60.
[21] J. P. Gisselbrecht, N. N. P. Moonen, C. Boudon, M. B. Nielsen, F. Diederich, M. Gross, *Eur. J. Org. Chem.* **2004**, 2959 – 2972.

